

# Accelerated optimization for dynamic MRI reconstruction with locally low-rank regularizers

J. Fessler  
LLR MR



Jeffrey A. Fessler

EECS Department, BME Department, Dept. of Radiology  
University of Michigan

<http://web.eecs.umich.edu/~fessler>

UM ECE CSP Seminar  
2024-01-18

Acknowledgments:

Caroline Crockett, Raj Nadakuditi, Rodrigo A. Lobos, Javier Salazar Cavazos

Introduction to dynamic imaging

Global low-rank methods

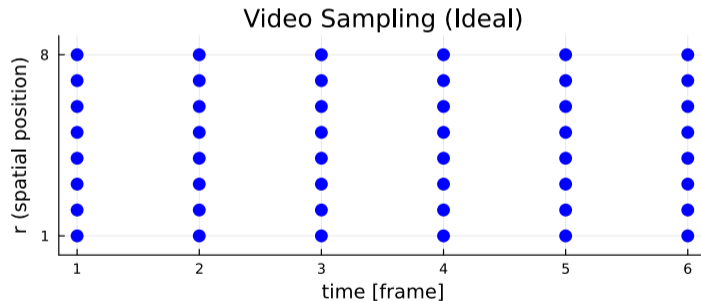
Local low-rank methods

Summary

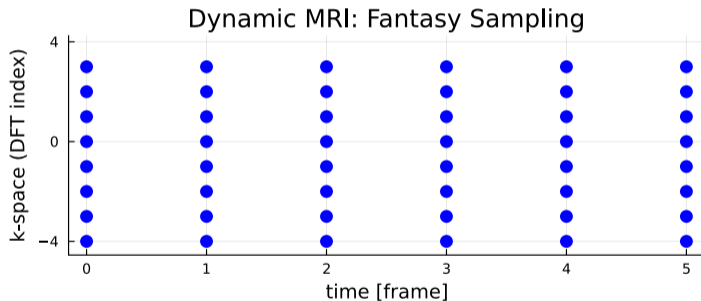
Bibliography

Backup figures

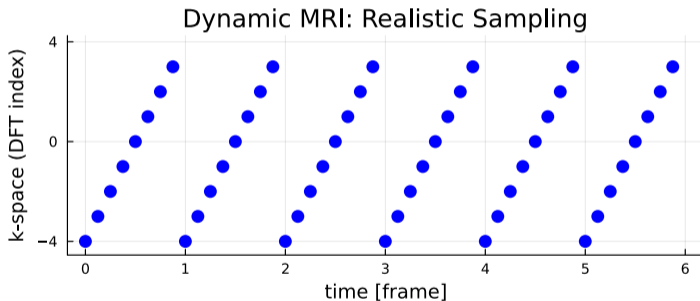
- ▶ Video: sampling in real space



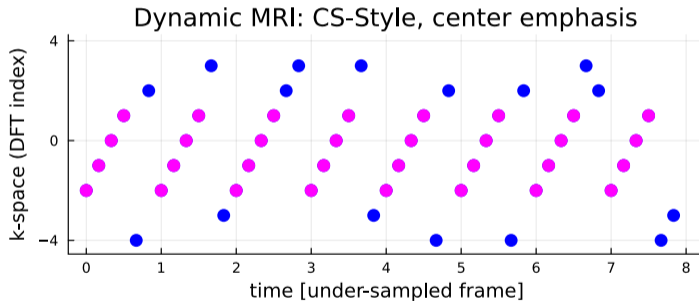
- ▶ MRI: sampling in k-space (k-t sampling)



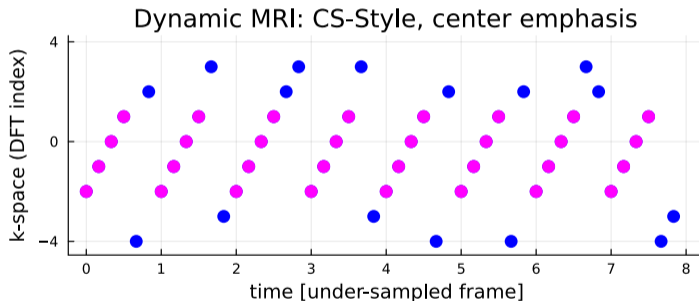
- MRI: sampling in k-space (k-t sampling)



- ▶ MRI: sampling in k-space (k-t sampling)



- ▶ MRI: sampling in k-space (k-t sampling)



- ▶ better temporal resolution, but under-sampled k-space

- ▶ Measurement model:

$$\mathbf{y}_t = \mathbf{A}_t \mathbf{x}_t + \boldsymbol{\varepsilon}_t, \quad t = 1, \dots, T$$

$\mathbf{y}_t \in \mathbb{C}^{M_t}$  : k-space data for  $t$ th frame

$\mathbf{x}_t \in \mathbb{C}^N$  : latent image for  $t$ th frame (vec of 2D or 3D array)

$\mathbf{A}_t \in \mathbb{C}^{M_t \times N}$  : forward model for  $t$ th frame

- ▶ Stack data:  $\mathbf{y} \triangleq \begin{bmatrix} \mathbf{y}_1 \\ \vdots \\ \mathbf{y}_T \end{bmatrix}$ ,  $\boldsymbol{\varepsilon} \triangleq \begin{bmatrix} \boldsymbol{\varepsilon}_1 \\ \vdots \\ \boldsymbol{\varepsilon}_T \end{bmatrix} \in \mathbb{C}^M$ ,  $M \triangleq \sum_{t=1}^T M_t$

- ▶ Latent space-time matrix  $\mathbf{X} \triangleq \begin{bmatrix} \mathbf{x}_1 & \dots & \mathbf{x}_T \end{bmatrix} \in \mathbb{C}^{N \times T}$

- ▶ Linear forward model:

$$\mathbf{y} = \mathcal{A}(\mathbf{X}) + \boldsymbol{\varepsilon}, \quad \mathcal{A} : \mathbb{C}^{N \times T} \mapsto \mathbb{C}^M$$

- ▶ Goal: estimate latent image sequence  $\mathbf{X}$  from data  $\mathbf{y}$  given  $\mathcal{A}$
- ▶ Under-determined  $M < N T$ , so regularization is essential



Introduction to dynamic imaging

Global low-rank methods

- Global nuclear norm

- L+S results

- Global LR results

- Smoothing

- Global LR smooth results

Local low-rank methods

Summary

Bibliography

Backup figures

If  $\mathbf{X}$  is assumed to be (globally) low-rank:

▶ rank constraint:

$$\hat{\mathbf{X}} = \arg \min_{\mathbf{X}} \frac{1}{2} \|\mathcal{A}(\mathbf{X}) - \mathbf{y}\|_2^2 \text{ such that } \text{rank}\{\mathbf{X}\} \leq K$$

▶ rank regularizer:

$$\hat{\mathbf{X}} = \arg \min_{\mathbf{X}} \frac{1}{2} \|\mathcal{A}(\mathbf{X}) - \mathbf{y}\|_2^2 + \beta \text{rank}\{\mathbf{X}\}$$

▶

If  $\mathbf{X}$  is assumed to be (globally) low-rank:

▶ rank constraint:

$$\hat{\mathbf{X}} = \arg \min_{\mathbf{X}} \frac{1}{2} \|\mathcal{A}(\mathbf{X}) - \mathbf{y}\|_2^2 \text{ such that } \text{rank}\{\mathbf{X}\} \leq K$$

▶ rank regularizer:

$$\hat{\mathbf{X}} = \arg \min_{\mathbf{X}} \frac{1}{2} \|\mathcal{A}(\mathbf{X}) - \mathbf{y}\|_2^2 + \beta \text{rank}\{\mathbf{X}\}$$

▶ Globally optimal SVD-based solutions *if*  $\mathcal{A} = \mathcal{I}$  or if  $\mathcal{A}$  is unitary, via Eckart-Young-Mirsky theorem

▶ Else, challenging non-convex problems

▶

If  $\mathbf{X}$  is assumed to be (globally) low-rank:

- ▶ rank constraint:

$$\hat{\mathbf{X}} = \arg \min_{\mathbf{X}} \frac{1}{2} \|\mathcal{A}(\mathbf{X}) - \mathbf{y}\|_2^2 \text{ such that } \text{rank}\{\mathbf{X}\} \leq K$$

- ▶ rank regularizer:

$$\hat{\mathbf{X}} = \arg \min_{\mathbf{X}} \frac{1}{2} \|\mathcal{A}(\mathbf{X}) - \mathbf{y}\|_2^2 + \beta \text{rank}\{\mathbf{X}\}$$

- ▶ Globally optimal SVD-based solutions *if*  $\mathcal{A} = \mathcal{I}$  or if  $\mathcal{A}$  is unitary, via Eckart-Young-Mirsky theorem
- ▶ Else, challenging non-convex problems
- ▶ Both “data driven:” temporal basis learned from data during reconstruction

- ▶ If  $\mathbf{X}$  is assumed to be (globally) low-rank:

$$\hat{\mathbf{X}} = \arg \min_{\mathbf{X}} \frac{1}{2} \|\mathcal{A}(\mathbf{X}) - \mathbf{y}\|_2^2 + \beta \|\mathbf{X}\|_*$$

$\|\mathbf{X}\|_*$  : nuclear norm



- ▶ If  $\mathbf{X}$  is assumed to be (globally) low-rank:

$$\hat{\mathbf{X}} = \arg \min_{\mathbf{X}} \frac{1}{2} \|\mathcal{A}(\mathbf{X}) - \mathbf{y}\|_2^2 + \beta \|\mathbf{X}\|_*$$

$\|\mathbf{X}\|_*$  : nuclear norm

- ▶ If  $\mathbf{X}$  is assumed to be (globally) low-rank + temporally sparse:

$$\hat{\mathbf{X}} = \hat{\mathbf{L}} + \hat{\mathbf{S}}, \quad (\hat{\mathbf{L}}, \hat{\mathbf{S}}) = \arg \min_{\mathbf{L}, \mathbf{S}} \frac{1}{2} \|\mathcal{A}(\mathbf{L} + \mathbf{S}) - \mathbf{y}\|_2^2 + \beta_1 \|\mathbf{L}\|_* + \beta_2 \|\mathbf{S}\mathbf{T}\|_{1,1}$$

for some temporal sparsifying transform  $\mathbf{T}$

$$\|\mathbf{X}\|_{1,1} \triangleq \|\text{vec}(\mathbf{X})\|_1$$



- ▶ If  $\mathbf{X}$  is assumed to be (globally) low-rank:

$$\hat{\mathbf{X}} = \arg \min_{\mathbf{X}} \frac{1}{2} \|\mathcal{A}(\mathbf{X}) - \mathbf{y}\|_2^2 + \beta \|\mathbf{X}\|_*$$

$\|\mathbf{X}\|_*$  : nuclear norm

- ▶ If  $\mathbf{X}$  is assumed to be (globally) low-rank + temporally sparse:

$$\hat{\mathbf{X}} = \hat{\mathbf{L}} + \hat{\mathbf{S}}, \quad (\hat{\mathbf{L}}, \hat{\mathbf{S}}) = \arg \min_{\mathbf{L}, \mathbf{S}} \frac{1}{2} \|\mathcal{A}(\mathbf{L} + \mathbf{S}) - \mathbf{y}\|_2^2 + \beta_1 \|\mathbf{L}\|_* + \beta_2 \|\mathbf{ST}\|_{1,1}$$

for some temporal sparsifying transform  $\mathbf{T}$

$$\|\mathbf{X}\|_{1,1} \triangleq \|\text{vec}(\mathbf{X})\|_1$$

- ▶ Both easily solved by proximal optimized gradient method (POGM)
  - (A. Taylor et al., SIAM JO, 2017) [1] with adaptive restart (D. Kim & JF, JOTA 2018) [2]
  - C. Lin & JF, IEEE T-CI 2019, [3]

- ▶ Composite cost function:

$$\hat{\mathbf{X}} = \arg \min_{\mathbf{X}} \Psi(\mathbf{X}), \quad \Psi(\mathbf{X}) = f(\mathbf{X}) + g(\mathbf{X}),$$

$$\underbrace{f(\mathbf{X}) = \frac{1}{2} \|\mathcal{A}(\mathbf{X}) - \mathbf{y}\|_2^2}_{\text{smooth}}, \quad \underbrace{g(\mathbf{X}) = \beta \|\mathbf{X}\|_*}_{\text{prox friendly}}, \quad \underbrace{L_{\nabla f} = \|\mathcal{A}^* \mathcal{A}\|_2}_{\text{Lipschitz constant}}$$

- ▶ Proximal gradient method (PGM) / Iterative soft thresholding algorithm (ISTA):

$$\mathbf{X}_{k+1} = \text{SVST}\left(\mathbf{X}_k - \frac{1}{L_{\nabla f}} \nabla f(\mathbf{X}_k), \frac{\beta}{L_{\nabla f}}\right), \quad \nabla f(\mathbf{X}_k) = \mathcal{A}^* (\mathcal{A}(\mathbf{X}_k) - \mathbf{y})$$

- ▶ Singular value soft thresholding (SVST):

$$\mathbf{X} = \mathbf{U} \text{Diag}\{\sigma_k\} \mathbf{V}' \implies \text{SVST}(\mathbf{X}, \gamma) = \text{prox}_{\gamma \|\cdot\|_*}(\mathbf{X}) = \mathbf{U} \text{Diag}\{[\sigma_k - \gamma]_+\} \mathbf{V}'$$

- ▶ FISTA and POGM are similar, with momentum terms



## OGM extension for composite problems by Taylor et al. [1]:

1306

A. B. TAYLOR, J. M. HENDRICKX, F. GLINEUR

### Proximal optimized gradient method (POGM)

Input:  $F^{(1)} \in \mathcal{F}_{0,L}(\mathbb{E})$ ,  $F^{(2)} \in \mathcal{F}_{0,\infty}(\mathbb{E})$ ,  $x_0 \in \mathbb{E}$ ,  $y_0 = x_0$ ,  $\theta_0 = 1$ .

For  $k = 1 : N$

$$y_k = x_{k-1} - \frac{1}{L} B^{-1} \nabla F^{(1)}(x_{k-1})$$

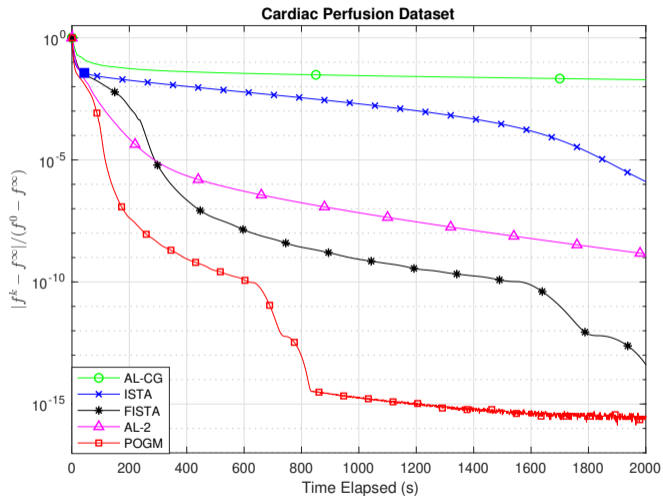
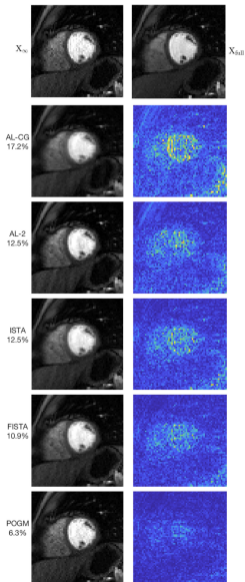
$$z_k = y_k + \frac{\theta_{k-1} - 1}{\theta_k} (y_k - y_{k-1}) + \frac{\theta_{k-1}}{\theta_k} (y_k - x_{k-1}) + \frac{\theta_{k-1} - 1}{L\gamma_{k-1}\theta_k} (z_{k-1} - x_{k-1})$$

$$x_k = \text{prox}_{\gamma_k F^{(2)}}(z_k)$$

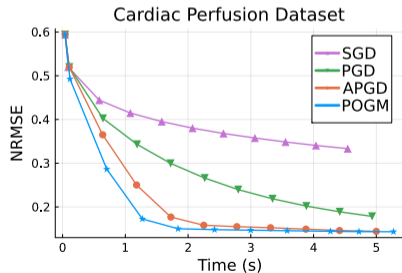
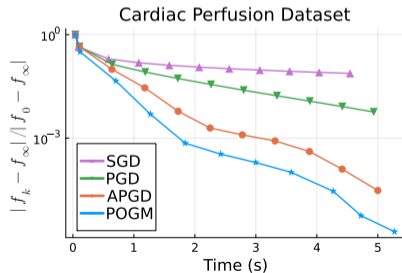
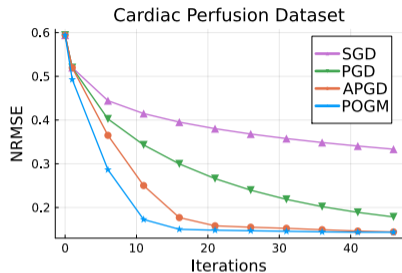
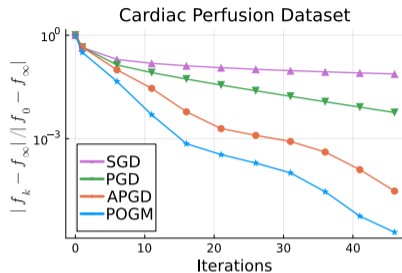
In this algorithm, we use the sequence  $\gamma_k = \frac{1}{L} \frac{2\theta_{k-1} + \theta_k - 1}{\theta_k}$  and the inertial coefficients proposed in [23]:

$$\theta_k = \begin{cases} \frac{1 + \sqrt{4\theta_{k-1}^2 + 1}}{2}, & i \leq N - 1, \\ \frac{1 + \sqrt{8\theta_{k-1}^2 + 1}}{2}, & i = N. \end{cases}$$

Simply trying to generalize OGM using the standard proximal step on the primary sequence  $\{y_i\}$  (as for FPGM1) does not lead to a converging algorithm. We obtained



C. Lin & JF, IEEE T-CI 2019 [3]. 12 coils, 10× under-sampling



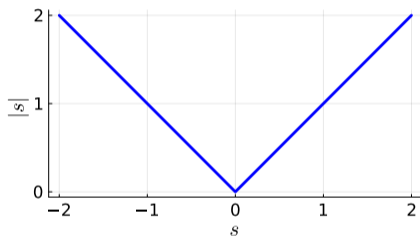
POGM works well in practice, corroborating “worst-case” bounds

- ▶ Nuclear norm regularizer is a non-smooth function of  $\mathbf{X}$ :

$$\|\mathbf{X}\|_* = \sum_k \sigma_k(\mathbf{X})$$

Singular value of  $1 \times 1$  matrix  $[s]$  is  $\sigma_1([s]) = |s|$

- ▶ Requires “complicated” methods like accelerated first-order proximal gradient methods, ADMM, ...
- ▶

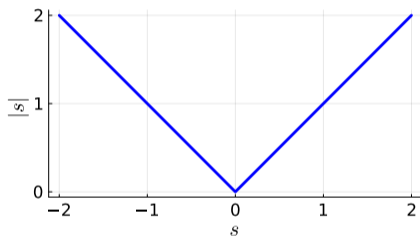


- ▶ Nuclear norm regularizer is a non-smooth function of  $\mathbf{X}$ :

$$\|\mathbf{X}\|_* = \sum_k \sigma_k(\mathbf{X})$$

Singular value of  $1 \times 1$  matrix  $[s]$  is  $\sigma_1([s]) = |s|$

- ▶ Requires “complicated” methods like accelerated first-order proximal gradient methods, ADMM, ...
- ▶  $\|\mathbf{X}\|_*$  is a relaxation of  $\text{rank}\{\mathbf{X}\}$

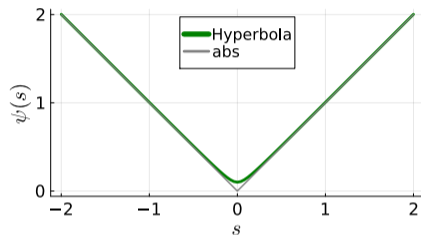


- ▶ Smooth regularizer:

$$R(\mathbf{X}) = \sum_k \psi(\sigma_k(\mathbf{X}))$$

- ▶ where  $\psi$  satisfies Huber's conditions [4]:

- $\psi(-s) = \psi(s)$
- $\psi$  differentiable
- $\omega_\psi(s) \triangleq \dot{\psi}(s) / s$  is bounded  
 $\implies \psi$  is Lipschitz



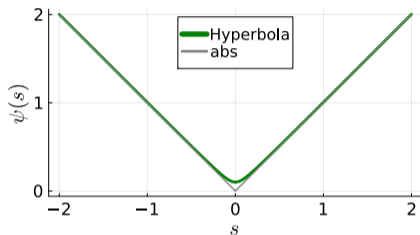
- ▶ hyperbola:  $\psi(s) = \sqrt{s^2 + \delta^2}$



- ▶ Smooth regularizer:

$$R(\mathbf{X}) = \sum_k \psi(\sigma_k(\mathbf{X}))$$

- ▶ where  $\psi$  satisfies Huber's conditions [4]:
  - $\psi(-s) = \psi(s)$
  - $\psi$  differentiable
  - $\omega_\psi(s) \triangleq \dot{\psi}(s) / s$  is bounded  
 $\implies \psi$  is Lipschitz
- ▶ Enables gradient-based optimization algorithms like nonlinear conjugate gradient (CG) and quasi-Newton
- ▶ Faster rate? [5]



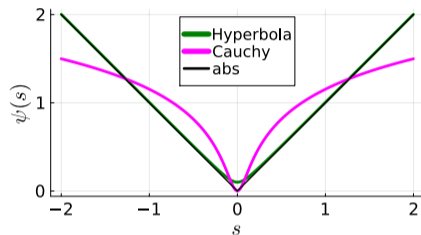
- ▶ hyperbola:  $\psi(s) = \sqrt{s^2 + \delta^2}$



- ▶ Smooth regularizer:

$$R(\mathbf{X}) = \sum_k \psi(\sigma_k(\mathbf{X}))$$

- ▶ where  $\psi$  satisfies Huber's conditions [4]:
  - $\psi(-s) = \psi(s)$
  - $\psi$  differentiable
  - $\omega_\psi(s) \triangleq \dot{\psi}(s)/s$  is bounded  
 $\implies \psi$  is Lipschitz
- ▶ Enables gradient-based optimization algorithms like nonlinear conjugate gradient (CG) and quasi-Newton
- ▶ Faster rate? [5]



- ▶ hyperbola:  $\psi(s) = \sqrt{s^2 + \delta^2}$
- ▶ Graduated non-convexity?



Smooth regularizer:

$$R(\mathbf{X}) = \sum_k \psi(\sigma_k(\mathbf{X}))$$

- ▶ **Convexity:**  $\psi$  convex  $\implies R$  convex [6]
- ▶ **Gradient:** (A. Lewis, J. Convex. Analysis, 1995) [7, 8]:

$$\begin{aligned}\mathbf{X} &= \mathbf{U} \text{Diag}\{\boldsymbol{\sigma}\} \mathbf{V}' \\ \implies \nabla R(\mathbf{X}) &= \mathbf{U} \text{Diag}\{\dot{\psi}(\boldsymbol{\sigma})\} \mathbf{V}'\end{aligned}$$



Smooth regularizer:

$$R(\mathbf{X}) = \sum_k \psi(\sigma_k(\mathbf{X}))$$

- ▶ **Convexity:**  $\psi$  convex  $\implies R$  convex [6]
- ▶ **Gradient:** (A. Lewis, J. Convex. Analysis, 1995) [7, 8]:

$$\begin{aligned}\mathbf{X} &= \mathbf{U} \text{Diag}\{\boldsymbol{\sigma}\} \mathbf{V}' \\ \implies \nabla R(\mathbf{X}) &= \mathbf{U} \text{Diag}\{\dot{\psi}(\boldsymbol{\sigma})\} \mathbf{V}'\end{aligned}$$

- ▶ **Smoothness Theorem:** Lipschitz constant

$$L_{\nabla R} = \omega_{\psi}(0) = \ddot{\psi}(0).$$

Proof builds on Qi & Yang, SIAM J. MAA 2003 [9]

- ▶ Smooth cost function:

$$\hat{\mathbf{X}} = \arg \min_{\mathbf{X}} \Psi(\mathbf{X}), \quad \Psi(\mathbf{X}) \triangleq \frac{1}{2} \|\mathcal{A}(\mathbf{X}) - \mathbf{y}\|_2^2 + \beta R(\mathbf{X}), \quad R(\mathbf{X}) = \sum_k \psi(\sigma_k(\mathbf{X}))$$

- ▶ Gradient (A. Lewis, J. Convex. Analysis, 1995) [7]:

$$\mathbf{X} = \mathbf{U} \text{Diag}\{\sigma_k\} \mathbf{V}' \implies \nabla \Psi(\mathbf{X}) = \mathcal{A}^* (\mathcal{A}(\mathbf{X}) - \mathbf{y}) + \beta \underbrace{\sum_k \dot{\psi}(\sigma_k(\mathbf{X})) \mathbf{u}_k \mathbf{v}_k'}_{\nabla R(\mathbf{X})}$$



- ▶ Smooth cost function:

$$\hat{\mathbf{X}} = \arg \min_{\mathbf{X}} \Psi(\mathbf{X}), \quad \Psi(\mathbf{X}) \triangleq \frac{1}{2} \|\mathcal{A}(\mathbf{X}) - \mathbf{y}\|_2^2 + \beta R(\mathbf{X}), \quad R(\mathbf{X}) = \sum_k \psi(\sigma_k(\mathbf{X}))$$

- ▶ Gradient (A. Lewis, J. Convex. Analysis, 1995) [7]:

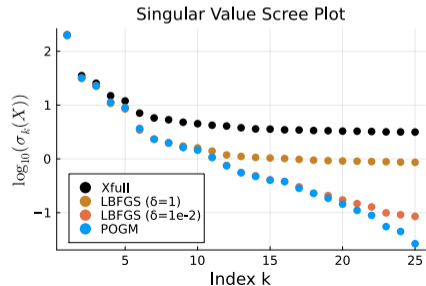
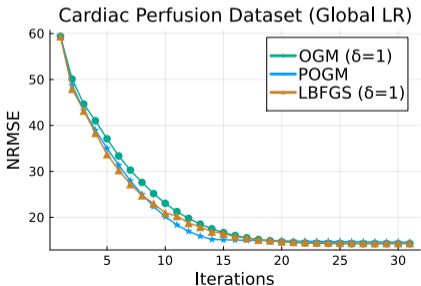
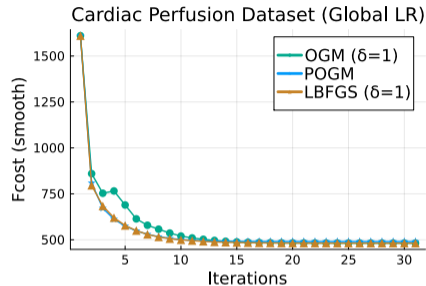
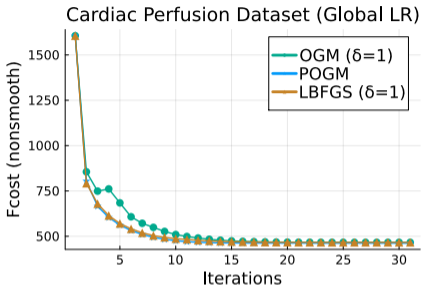
$$\mathbf{X} = \mathbf{U} \text{Diag}\{\sigma_k\} \mathbf{V}' \implies \nabla \Psi(\mathbf{X}) = \mathcal{A}^* (\mathcal{A}(\mathbf{X}) - \mathbf{y}) + \beta \underbrace{\sum_k \dot{\psi}(\sigma_k(\mathbf{X})) \mathbf{u}_k \mathbf{v}_k'}_{\nabla R(\mathbf{X})}$$

- ▶ Line search function (for step size):

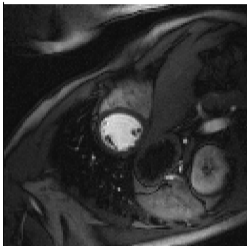
$$h(\alpha) \triangleq \Psi(\mathbf{X} + \alpha \Delta), \quad \dot{h}(\alpha) = \mathcal{A}(\Delta)' (\mathcal{A}(\mathbf{X} + \alpha \Delta) - \mathbf{y}) + \beta \langle \nabla R(\mathbf{X} + \alpha \Delta), \Delta \rangle_{\text{F}}$$

- ▶ **Theorem:**  $h$  is smooth;  $\dot{h}$  has Lipschitz constant

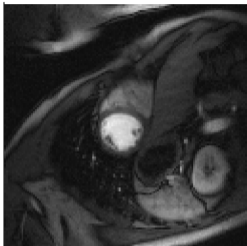
$$L_{\dot{h}} = \|\mathcal{A}(\Delta)\|_2^2 + \beta \omega_{\psi}(0) \|\Delta\|_{\text{F}}^2$$



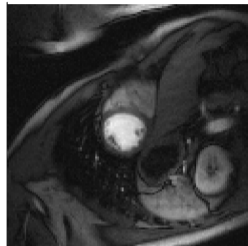
Fully Sampled Ref.



POGM - NRMSE: 14.6 %



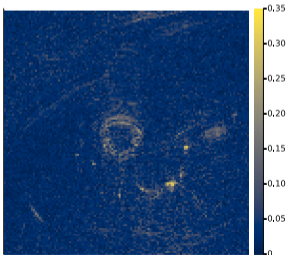
LBFGS - NRMSE: 14.4 %



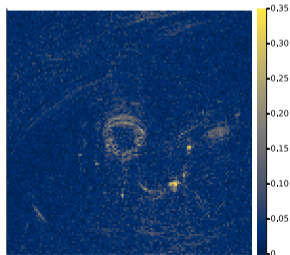
Initial Image



POGM - NRMSE: 14.6 %



LBFGS - NRMSE: 14.4 %



Introduction to dynamic imaging

Global low-rank methods

Local low-rank methods

- Low-rank local patches

- Overlapping patches

- Smooth regularizer

- LLR results

Summary

Bibliography

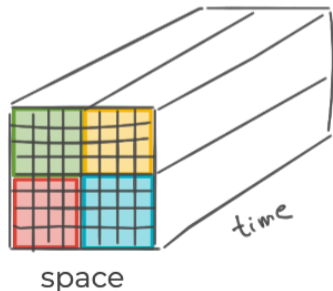
Backup figures

- ▶ If space-time patches of  $\mathbf{X}$  are assumed to be (locally) low-rank:

$$\hat{\mathbf{X}} = \arg \min_{\mathbf{X}} \frac{1}{2} \|\mathcal{A}(\mathbf{X}) - \mathbf{y}\|_2^2 + \beta \sum_{p=1}^P \|\mathcal{P}_p(\mathbf{X})\|_*$$

$\mathcal{P}_p$ : picks the  $p$ th space-time patch from  $\mathbf{X}$

- ▶ Low-rank modeling may be more reasonable locally





- ▶ If space-time patches of  $\mathbf{X}$  are assumed to be (locally) low-rank:

$$\hat{\mathbf{X}} = \arg \min_{\mathbf{X}} \frac{1}{2} \|\mathcal{A}(\mathbf{X}) - \mathbf{y}\|_2^2 + \beta \sum_{p=1}^P \|\mathcal{P}_p(\mathbf{X})\|_*$$

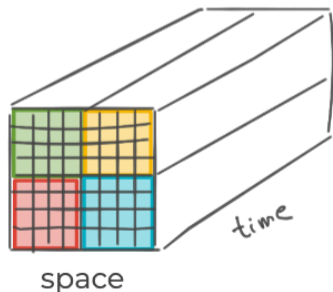
$\mathcal{P}_p$ : picks the  $p$ th space-time patch from  $\mathbf{X}$

- ▶ Low-rank modeling may be more reasonable locally



Numerous applications, e.g.:

- matrix approximation [10]
- dynamic MRI [11, 12]
- multi-contrast and quantitative MRI [13–15]
- MR denoising [16]
- MR motion correction [17]
- fMRI denoising [18–20]
- fMRI dynamic image reconstruction [21]



$$\hat{\mathbf{X}} = \arg \min_{\mathbf{X}} \frac{1}{2} \|\mathcal{A}(\mathbf{X}) - \mathbf{y}\|_2^2 + \beta \sum_{p=1}^P \|\mathcal{P}_p(\mathbf{X})\|_*$$

- ▶ Non-overlapping patches
  - prox-friendly: separate SVST for each space-time patch
  - Suitable for proximal gradient methods like POGM *only* in this case
- ▶

$$\hat{\mathbf{X}} = \arg \min_{\mathbf{X}} \frac{1}{2} \|\mathcal{A}(\mathbf{X}) - \mathbf{y}\|_2^2 + \beta \sum_s \sum_{p=1}^P \|\mathcal{P}_p(\text{Shift}_s(\mathbf{X}))\|_*$$

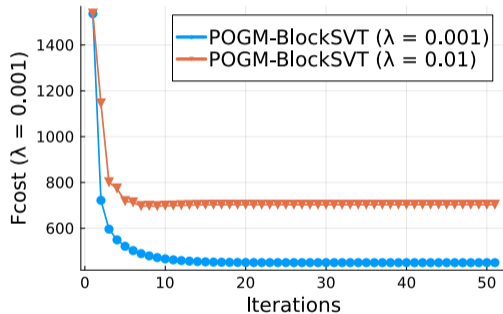
- ▶ Non-overlapping patches
  - prox-friendly: separate SVST for each space-time patch
  - Suitable for proximal gradient methods like POGM *only* in this case
- ▶ Overlapping patches (stride < patch size)
  - shift invariant (if stride = 1)  $\implies$  no block artifacts
  - no (known) simple proximal operator
  -

$$\hat{\mathbf{X}} = \arg \min_{\mathbf{X}} \frac{1}{2} \|\mathcal{A}(\mathbf{X}) - \mathbf{y}\|_2^2 + \beta \sum_s \sum_{p=1}^P \|\mathcal{P}_p(\text{Shift}_s(\mathbf{X}))\|_*$$

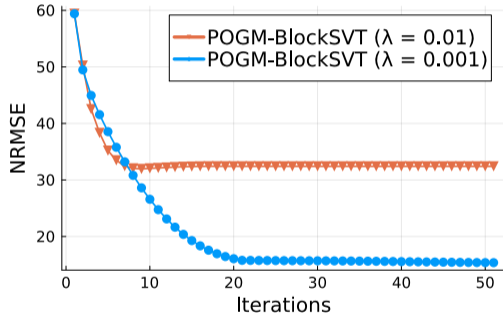
- ▶ Non-overlapping patches
  - prox-friendly: separate SVST for each space-time patch
  - Suitable for proximal gradient methods like POGM *only* in this case
- ▶ Overlapping patches (stride < patch size)
  - shift invariant (if stride = 1)  $\implies$  no block artifacts
  - no (known) simple proximal operator
  - Optimization algorithm options:
    - ▶ subgradient descent
    - ▶ cycle spinning approximation (akin to stochastic proximal gradient method)
    - ▶ proximal averaging [22, 23]: prox of sum  $\approx$  sum of prox ?
    - ▶ ADMM with *numerous* auxiliary variables, cf. [24, 25]



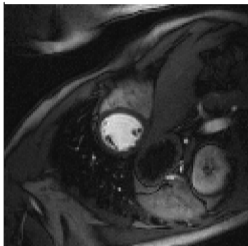
### Cardiac Perfusion - LLR Results



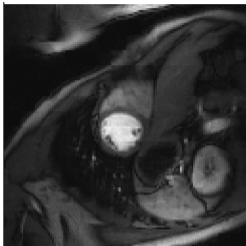
### Cardiac Perfusion - LLR Results



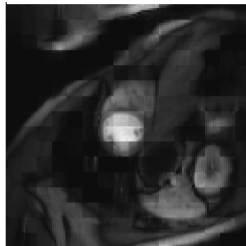
Fully Sampled Ref.



POGM ( $\lambda = 0.001$ )



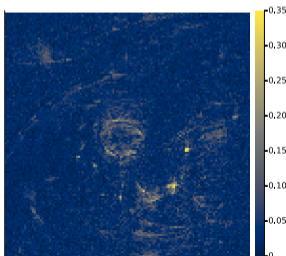
POGM ( $\lambda = 0.01$ )



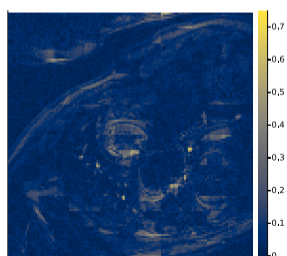
Initial Image

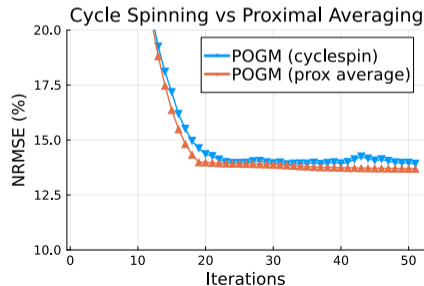
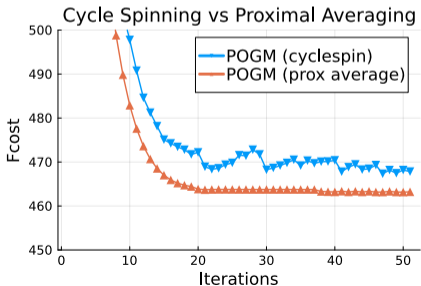
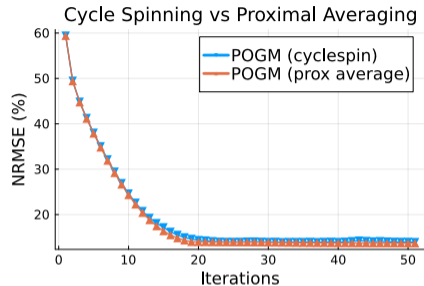
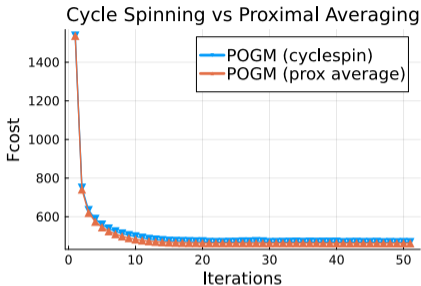


POGM - NRMSE: 15.4 %

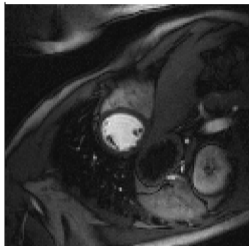


POGM - NRMSE: 32.4 %





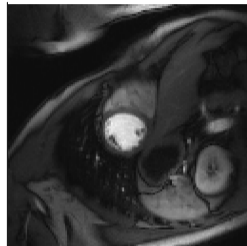
Fully Sampled Ref.



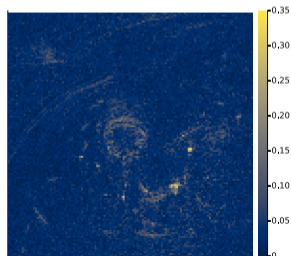
Initial Image



POGM - NRMSE 13.7 %



POGM - NRMSE 13.7 %





$$\hat{\mathbf{X}} = \arg \min_{\mathbf{X}} \Psi(\mathbf{X}), \quad \Psi(\mathbf{X}) \triangleq \frac{1}{2} \|\mathcal{A}(\mathbf{X}) - \mathbf{y}\|_2^2 + \beta \sum_{p=1}^P R_p(\mathbf{X}), \quad R_p(\mathbf{X}) \triangleq \sum_k \psi(\sigma_k(\mathcal{P}_p(\mathbf{X})))$$

Now we can easily apply gradient-based methods like CG & quasi-Newton:

- ▶ Gradient (corollary to previous theorem):

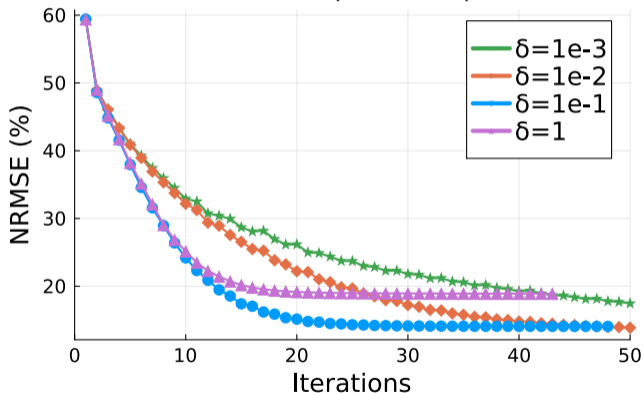
$$\nabla \Psi(\mathbf{X}) = \mathcal{A}^*(\mathcal{A}(\mathbf{X}) - \mathbf{y}) + \beta \sum_{p=1}^P \mathcal{P}_p^* \left( \mathbf{U}_p \text{Diag} \left\{ \dot{\psi}(\sigma_p) \right\} \mathbf{V}_p' \right), \quad \mathcal{P}_p(\mathbf{X}) = \mathbf{U}_p \text{Diag} \{ \sigma_p \} \mathbf{V}_p'$$

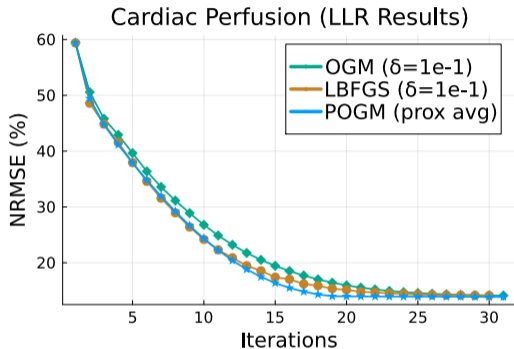
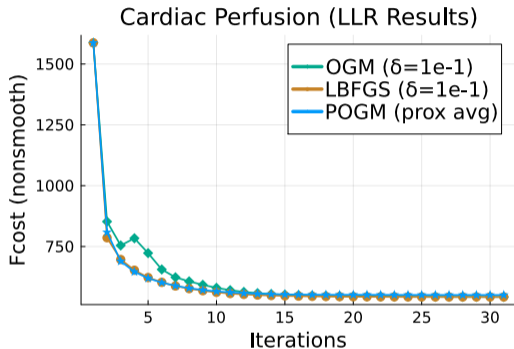
- ▶ Lipschitz constant (for line-search step):

$$L_{\nabla \Psi} = \|\mathcal{A}^* \mathcal{A}\|_2 + \beta P \omega_{\psi}(0)$$

$$L_h = \|\mathcal{A}(\Delta)\|_2^2 + \beta \omega_{\psi}(0) \sum_{p=1}^P \|\mathcal{P}_p(\Delta)\|_{\text{F}}^2 \leq L_{\nabla \Psi} \|\Delta\|_{\text{F}}^2.$$

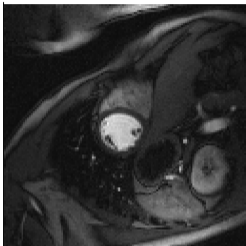
Hyperbola potential function:  $\psi(\sigma) = \sqrt{\sigma^2 + \delta^2} \approx |\sigma|$  for  $|\sigma| \gg \delta$   
 LBFGS ( $\lambda=0.001$ )



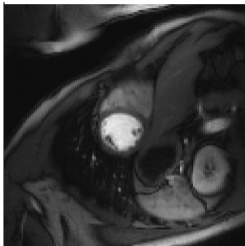


- ▶ POGM with proximal averaging descends, but to what?
- ▶ Room to optimize LBFGS

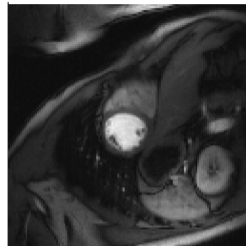
Fully Sampled Ref.



POGM - NRMSE: 13.9 %



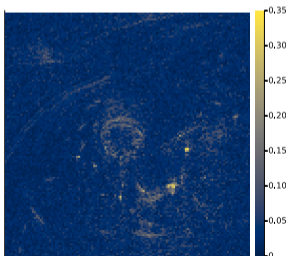
LBFGS - NRMSE: 14.1 %



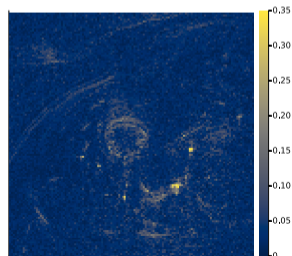
Initial Image



POGM - NRMSE: 13.9 %



LBFGS - NRMSE: 14.1 %



Introduction to dynamic imaging

Global low-rank methods

Local low-rank methods

**Summary**

Bibliography

Backup figures



- ▶ Smooth approximation to nuclear norm
  - leads to similar dynamic image reconstruction results
  - Lipschitz gradient enables efficient convex optimization with convergence
  - POGM with cycle-spinning or proximal averaging works unexpectedly well but what convergence theory?
- ▶

- ▶ Smooth approximation to nuclear norm
  - leads to similar dynamic image reconstruction results
  - Lipschitz gradient enables efficient convex optimization with convergence
  - POGM with cycle-spinning or proximal averaging works unexpectedly well but what convergence theory?
- ▶ Future
  - ▶ Non-convexity
    - Non-convex  $\psi$ , e.g., [24, 25]
    - Regularize tail singular values [26]:  $R(\mathbf{X}) = \sum_{k=\hat{r}+1} \psi(\sigma_k(\mathbf{X}))$
  - ▶ Reduce computation time
    - Quadratic majorizer for better line search?
    - Exploit parallelism in code
    - Inter-twine Newton-like methods with proximal methods? [27]
    - Iteration-dependent regularization parameter? [13]
    - Compare POGM with OptISTA [28]

Talk and code available online at  
<http://web.eecs.umich.edu/~fessler>



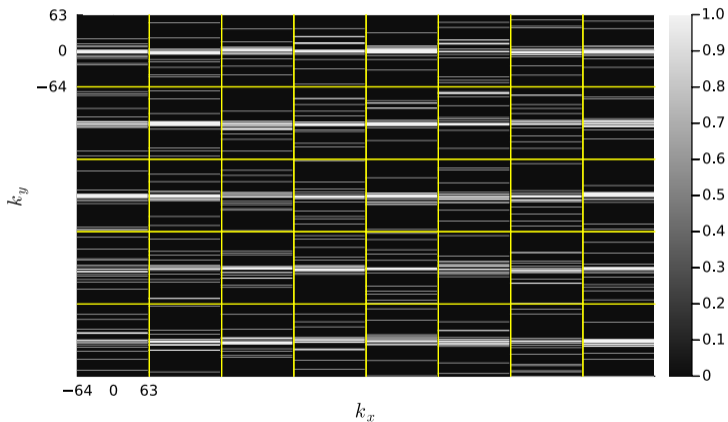


- [1] A. B. Taylor, J. M. Hendrickx, and Francois Glineur. "Exact worst-case performance of first-order methods for composite convex optimization." In: *SIAM J. Optim.* 27.3 (Jan. 2017), 1283–313.
- [2] D. Kim and J. A. Fessler. "Adaptive restart of the optimized gradient method for convex optimization." In: *J. Optim. Theory Appl.* 178.1 (July 2018), 240–63.
- [3] C. Y. Lin and J. A. Fessler. "Efficient dynamic parallel MRI reconstruction for the low-rank plus sparse model." In: *IEEE Trans. Computational Imaging* 5.1 (Mar. 2019), 17–26.
- [4] P. J. Huber. *Robust statistics*. New York: Wiley, 1981.
- [5] A. I. Cohen. "Rate of convergence of several conjugate gradient algorithms." In: *SIAM J. Numer. Anal.* 9.2 (1972), 248–59.
- [6] C. Davis. "All convex invariant functions of Hermitian matrices." In: *Archiv der Mathematik* 8.4 (1957), 276–8.
- [7] A. S. Lewis. "The convex analysis of unitarily invariant matrix functions." In: *J. Convex Analysis* 2.1 (1995), 173–83.
- [8] A. S. Lewis. "Derivatives of spectral functions." In: *Mathematics of Operations Research* 21.3 (1996), 576–88.
- [9] H. Qi and X. Yang. "Semismoothness of spectral functions." In: *SIAM J. Matrix. Anal. Appl.* 25.3 (2003), 766–83.
- [10] J. Lee, S. Kim, G. Lebanon, and Y. Singer. "Local low-rank matrix approximation." In: *Proc. Intl. Conf. Mach. Learn.* Vol. 28. 2013, 82–90.
- [11] J. Trzasko and A. Manduca. "Local versus global low-rank promotion in dynamic MRI series reconstruction." In: *Proc. Intl. Soc. Mag. Res. Med.* 2011, p. 4371.
- [12] Z. Ke, W. Huang, Z-X. Cui, J. Cheng, S. Jia, H. Wang, X. Liu, H. Zheng, L. Ying, Y. Zhu, and D. Liang. "Learned low-rank priors in dynamic MR imaging." In: *IEEE Trans. Med. Imag.* 40.12 (2021), 3698–710.
- [13] T. Zhang, J. M. Pauly, and I. R. Levesque. "Accelerating parameter mapping with a locally low rank constraint." In: *Mag. Res. Med.* 73.2 (2015), 655–61.

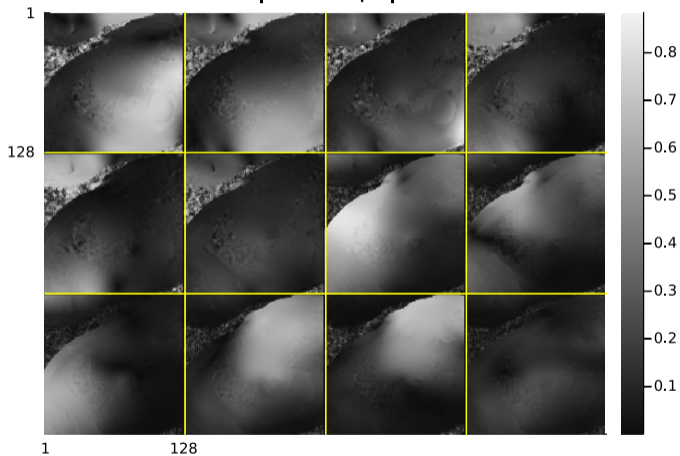
- [14] B. Yaman, S. Weingartner, N. Kargas, N. D. Sidiropoulos, and M. Akcakaya. "Locally low-rank tensor regularization for high-resolution quantitative dynamic MRI." In: *Proc. Intl. Wkshp. Comp. Adv. Multi-Sensor Adapt. Proc.* 2017.
- [15] J. I. Tamir, M. Uecker, W. Chen, P. Lai, M. T. Alley, S. S. Vasanawala, and M. Lustig. "T2 shuffling: sharp, multicontrast, volumetric fast spin-echo imaging." In: *Mag. Res. Med.* 77.1 (Jan. 2017), 180–95.
- [16] J. Lu, C. Xu, Z. Hu, X. Liu, Q. Jiang, D. Meng, and Z. Lin. "A new nonlocal low-rank regularization method with applications to magnetic resonance image denoising." In: *Inverse Prob.* 38.6 (May 2022), p. 065012.
- [17] X. Chen et al. "Improved structured low-rank reconstruction for 3D multi-shot EPI with joint motion modelling." In: *ISMRM Workshop on Data Sampling and Image Reconstruction*. 2023.
- [18] L. Vizioli, S. Moeller, L. Dowdle, M. Akcakaya, F. D. Martino, E. Yacoub, and K. Ugurbil. "Lowering the thermal noise barrier in functional brain mapping with magnetic resonance imaging." In: *Nature Comm.* 12 (2021), p. 5181.
- [19] P-A. Comby, Z. Amor, A. Vignaud, and P. Ciuciu. "Denoising of fMRI volumes using local low rank methods." In: *Proc. IEEE Intl. Symp. Biomed. Imag.* 2023.
- [20] N. K. Meyer, D. Kang, D. F. Black, N. G. Campeau, K. M. Welker, E. M. Gray, M-H. In, Y. Shu, J. Huston, M. A. Bernstein, and J. D. Trzasko. "Enhanced clinical task-based fMRI metrics through locally low-rank denoising of complex-valued data." In: *The Neuroradiology J.* 36.3 (June 2023), 273–88.
- [21] S. Guo, J. A. Fessler, and D. C. Noll. "High-resolution oscillating steady-state fMRI using patch-tensor low-rank reconstruction." In: *IEEE Trans. Med. Imag.* 39.12 (Dec. 2020), 4357–68.
- [22] H. Bauschke, R. Goebel, Y. Lucet, and X. Wang. "The proximal average: basic theory." In: *SIAM J. Optim.* 19.2 (2008), 766–85.
- [23] L. W. Zhong and J. T. Kwok. "Accelerated stochastic gradient method for composite regularization." In: *AISTATS*. 2014, 1086–94.
- [24] Z. Kang, C. Peng, and Q. Cheng. "Robust subspace clustering via smoothed rank approximation." In: *IEEE Signal Proc. Letters* 22.11 (2015), 2088–92.

- [25] M. Azghani, A. Esmaili, K. Behdin, and F. Marvasti. "Missing low-rank and sparse decomposition based on smoothed nuclear norm." In: *ieee-csvt* 30.6 (2020), 1550–8.
- [26] J. A. S. Cavazos, J. A. Fessler, and L. Balzano. "Sample-wise heteroscedastic PCA with tail singular value regularization." In: *Proc. IEEE Intl. Conf. on Sampling Theory and Appl. (SampTA)*. 2023, 1–6.
- [27] G. Bareilles, F. Iutzeler, and Jerome Malick. "Newton acceleration on manifolds identified by proximal gradient methods." In: *Mathematical Programming* 200 (2023), 37–70.
- [28] U. Jang, S. D. Gupta, and E. K. Ryu. *Computer-assisted design of accelerated composite optimization methods: optISTA*. 2023.

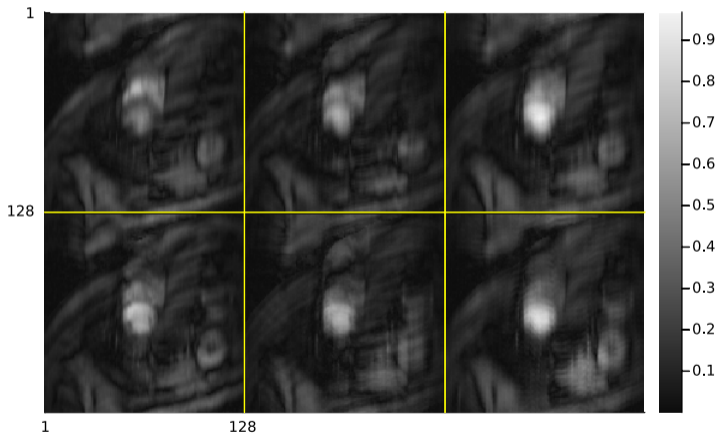
Sampling patterns for 40 frames; R8



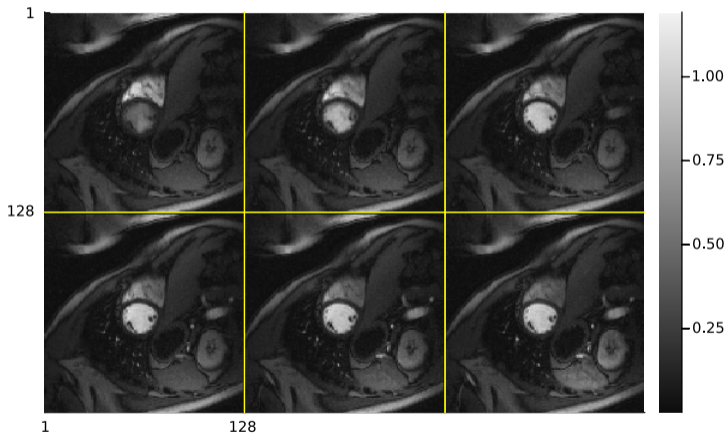
Normalized |coil maps| for 12 coils



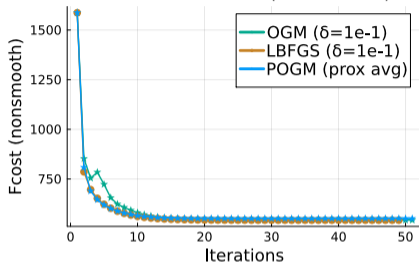
|Initial L|



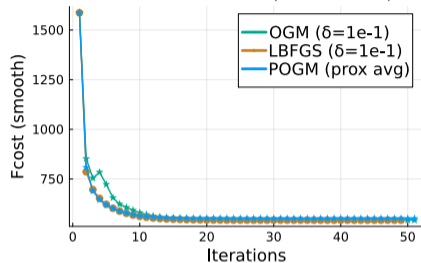
|Fully Sample X, Xfull|



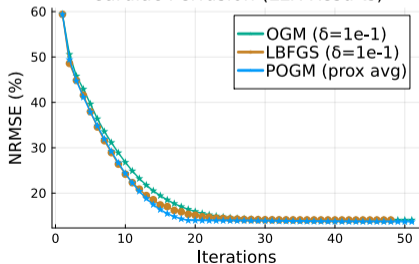
Cardiac Perfusion (LLR Results)



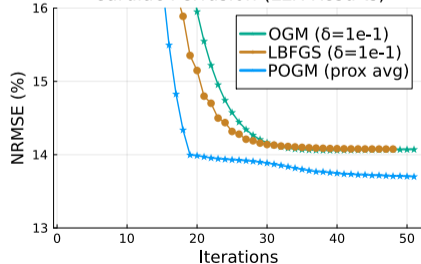
Cardiac Perfusion (LLR Results)



Cardiac Perfusion (LLR Results)



Cardiac Perfusion (LLR Results)





OGM - NRMSE: 14.1 %



OGM - NRMSE: 14.1 %

